

## X-ray-induced thinning of $^3\text{He}$ and $^3\text{He}/^4\text{He}$ mixture films

Konstantin Penanen,\* Masafumi Fukuto, Isaac F. Silvera, and Peter S. Pershan  
*Department of Physics, Harvard University, Cambridge, Massachusetts 02138*

(Received 22 February 2000)

Films of isotopic mixtures of helium have been studied using x-ray specular reflectivity techniques. In contrast with superfluid  $^4\text{He}$  films, x-ray exposure causes a reduction in the thickness of  $^4\text{He}$  films above the superfluid transition as well as films of pure  $^3\text{He}$  and  $^3\text{He}/^4\text{He}$  mixtures. One proposed model that could account for this effect is a charging model, in which thinning is caused by electrostatic pressure of free charges that accumulate on the helium surface. Unfortunately, this model is not fully consistent with all of the experimental observations. A localized heating model, in which indirect heating of the film causes it to thin would explain the data if there were dissipative film flow in the  $^3\text{He}/^4\text{He}$  mixtures at temperatures where the bulk is superfluid. We argue that various published experimental results suggest such an effect. In this model, film thinning data for dilute  $^3\text{He}/^4\text{He}$  films indicates dissipation that is linear in  $^3\text{He}$  content of the film over two orders of magnitude.

### I. INTRODUCTION

The method of x-ray specular reflectivity has been used successfully as a probe of surface structure in a variety of experimental systems, including studies of superfluid helium films (for a more detailed review of the method and the experimental setup see Ref. 1). For pure  $^4\text{He}$  films the method has been successful at temperatures where the bulk phase is superfluid and it has been possible to measure the liquid/vapor interface for films of various thicknesses adsorbed on the Si(111) face. On the other hand, exposure to x rays will sometimes induce changes in the quantities being measured and this unwanted effect has been observed for different thin helium films. For example, x rays induce thinning of  $^4\text{He}$  films above the superfluid transition.<sup>2,3</sup> In addition we found similar effects in films of pure  $^3\text{He}$  and  $^3\text{He}/^4\text{He}$  isotopic mixtures at temperatures where the bulk mixtures were in the normal state as well as at temperatures where they were expected to be superfluid. In fact, for  $^3\text{He}/^4\text{He}$  mixtures containing greater than 10%  $^3\text{He}$  the effect was sufficiently large for even very small x-ray exposures that it could not be easily quantified. The same is true for pure  $^4\text{He}$  films above the superfluid transition.

An overview of the experimental data follows. A theoretical overview of the two proposed models is given in the discussion section.

### II. THINNING OF HELIUM FILMS—EXPERIMENTAL DATA

#### A. Films of $^3\text{He}/^4\text{He}$ mixtures

By working with small amounts of  $^3\text{He}$  in the cell, we were able to take specular reflectivity measurements where the extent of thinning was small and could be quantified. Two types of measurements were performed. Results of conventional x-ray reflectivity measurements ( $R/R_F$  vs  $q_z$ ) that are shown in Fig. 1 and summarized in Table I illustrate that the thinning effect is related to the x-ray dosage per unit area. For fixed beam height, the area of exposed surface decreases with increasing incident angle such that for a fixed incident

intensity the intensity per unit area of exposed surface increases. As can be seen in Fig. 1 the period of the interference oscillations increases with increasing  $q_z$ , implying the film thickness decreases with increasing  $q_z$ . Furthermore, it is also apparent that the thinning is larger when the overall content of  $^3\text{He}$  is also larger.

In the second type of measurement, the reflectivity was measured at fixed angle, or constant  $q_z$ , as a function of temperature. In these measurements, variations in the reflected intensity indicate changes in the film thickness. An illustration of this method is shown in Fig. 2. Measurements of constant  $q_z$  reflectivity as a function of the cell temperature for different  $^3\text{He}$  content in the cell and different incident x-ray intensities are shown in Fig. 3. As the temperature is lowered, the film thickness first increases due to condensation of  $^4\text{He}$ . By  $T \approx 0.65$  K the amount of  $^4\text{He}$  in the vapor

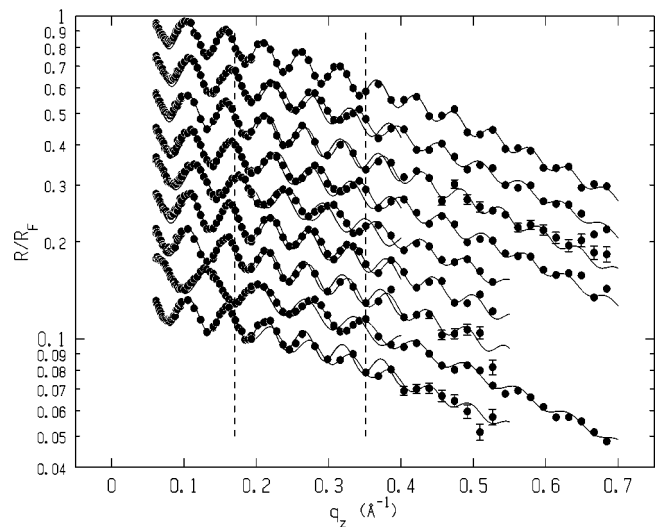


FIG. 1. Reflectivity normalized to silicon Fresnel reflectivity for a set of  $^3\text{He}/^4\text{He}$  mixtures. Film thickness for each data set is fit in the ranges  $0.12$ – $0.22 \text{ \AA}^{-1}$  (darker line) and  $0.3$ – $0.4 \text{ \AA}^{-1}$  (lighter line). The data correspond to the temperatures and concentrations listed in Table I. They are offset vertically in the same order as they appear in the table.

TABLE I. Thinning effect for dilute  $^3\text{He}/^4\text{He}$  mixtures. The amount of  $^4\text{He}$  in the cell is the same for all data sets. Incident flux (direct beam) is the monitor count $\times 117\,000$ . It corresponds to total energy flux reaching the detector of  $1.16\times 10^{13}$  eV/sec, or  $1.86\ \mu\text{W}$  at a monitor count of 10 000. Corrected for absorption in the output cryostat windows, and the detector efficiency (0.8 each), the energy flux incident on the substrate is  $\approx 2.9\ \mu\text{W}$ . Wave vector  $q_z$  of  $0.35\ \text{\AA}^{-1}$  corresponds to incident angle  $\theta=2^\circ$ . The typical error in thickness fits over a small fitting range is  $\pm 0.5\ \text{\AA}$  for sets without absorber;  $\pm 1\ \text{\AA}$  with  $\times 0.102$  absorber (\*).

$T$ K	% $^3\text{He}$	Eff. monitor	$d@0.17\ \text{\AA}^{-1}$	$\Delta d$	$d@0.35\ \text{\AA}^{-1}$	$\Delta d$
0.492	0	6600	119.53	0	119.47	0
0.491	0.8	960*	118.78	0.75	116.79	2.68
0.440	0.8	710*	117.83	1.70	115.19	4.28
0.452	2.3	470*	117.73	1.80	114.05	5.42
0.519	0.8	6950	115.51	4.02	112.78	6.69
0.491	0.8	5800	114.08	5.45	110.82	8.65
0.491	0.8	7200	113.57	5.96	109.82	9.65
0.440	0.8	7100	107.04	12.49	102.53	16.94
0.440	2.3	11750	93.13	26.4	89.35	30.12

becomes negligible and for pure  $^4\text{He}$  film the thickness stops changing. However, if the cell is loaded even with a small amount of  $^3\text{He}$ , the thickness dependence becomes abnormal: the film gets thinner at lower temperatures. The extent of thinning, just as in conventional reflectivity measurements, is larger for lower temperatures, higher overall  $^3\text{He}$  content and larger x-ray flux.

The model used to fit data in for the anomalous thinning effect illustrated in Fig. 3 assumes that for a given x-ray intensity the extent of thinning is proportional to the amount of  $^3\text{He}$  in the film. Taking the saturated vapor pressure for  $^3\text{He}$   $P_{\text{sat}}=P_{\text{sat}}(T)$ , the amount of  $^3\text{He}$  in the film can be estimated from the equilibrium chemical potential. In the film,

$$\mu_{\text{film}}=kT \ln \frac{N_{\text{film}}}{N_{\text{sat}}}, \quad (1)$$

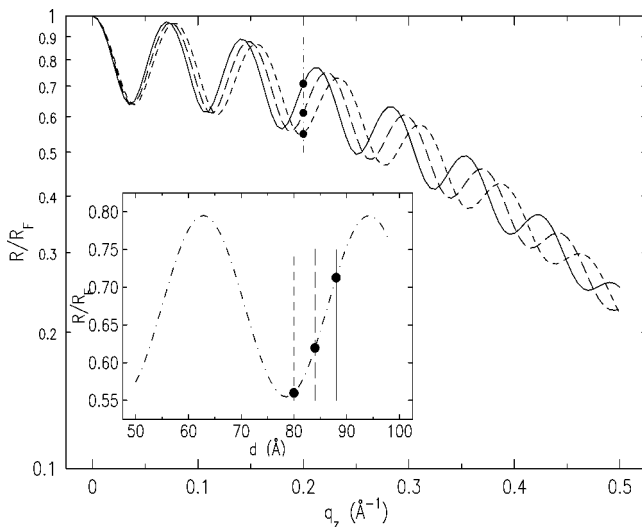


FIG. 2. An illustration of constant  $q_z$  x-ray reflectivity measurements. The plot shows the calculated normalized reflectivity as a function of wave vector transfer  $q_z$  for three film thicknesses: (—) 88 Å, (---) 84 Å, and (-·-·-) 80 Å. The inset shows the calculated reflectivity at constant  $q_z=0.2\ \text{\AA}^{-1}$  as a function of the film thickness.

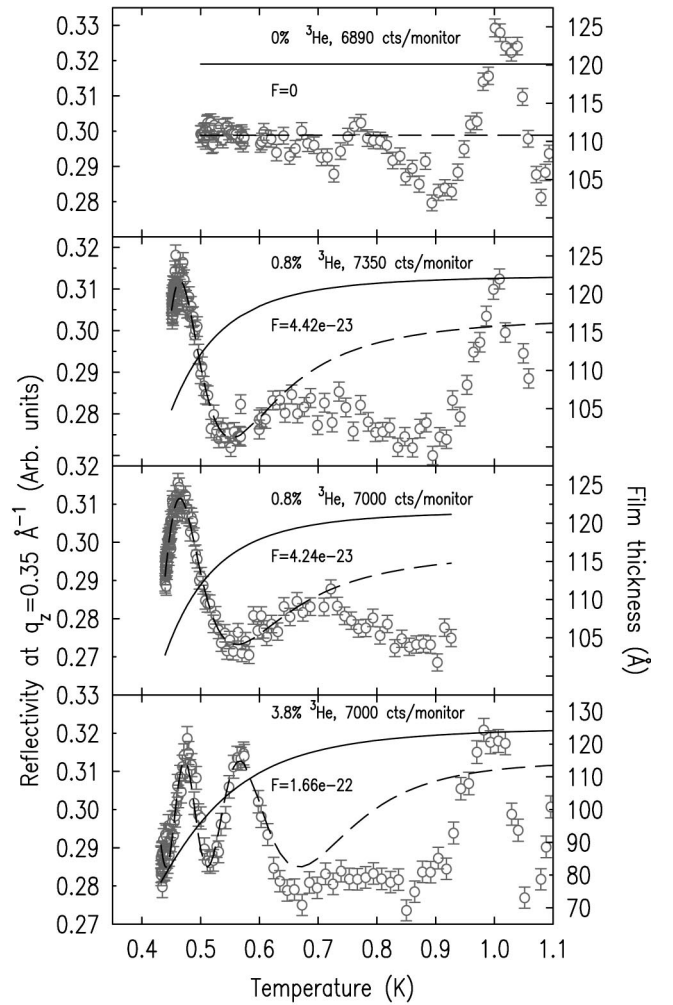


FIG. 3. Reflectivity at constant  $q_z=0.35\ \text{\AA}^{-1}$  as a function of temperature for different x-ray intensities and  $^3\text{He}$  content in the cell. --- Fit to reflectivity. — Film thickness vs temperature from fit (right axis). Deviations at  $T>0.7$  K are due to  $^4\text{He}$  evaporating from the film into the gas phase. The factor  $F$  refers to the multiplicative factor in the model for the anomalous thinning behavior for  $T<0.7$  K (see text).

where  $N_{\text{film}}$  is the content of  $^3\text{He}$  in the film and  $N_{\text{sat}}$  is a parameter. In the gas phase

$$\mu_{\text{vapor}} = kT \ln \frac{P}{P_{\text{sat}}}. \quad (2)$$

Assuming that the amount of  $^3\text{He}$  in the film remains small in comparison with the amount of  $^3\text{He}$  in the gas phase, the pressure  $P = \text{const} \times T$ . The concentration of  $^3\text{He}$  in the film is then

$$N_{\text{film}} = N_{\text{sat}} \frac{P}{P_{\text{sat}}} = \text{const} \times N_{\text{sat}} \frac{T}{P_{\text{sat}}}. \quad (3)$$

Equation (3) is valid as long as  $N_{\text{sat}}$  is a much weaker function of temperature than  $P_{\text{sat}}$ . The dependence of  $^3\text{He}$  saturated vapor pressure  $P_{\text{sat}}$  on temperature was fit to published data (Ref. 4, and references therein). For larger changes in the film thickness, the amount of thinning can be estimated from the change in the local  $^4\text{He}$  chemical potential, which scales as  $d^{-3}$ . The net result is that the film thickness should scale as

$$\frac{1}{d^3} - \frac{1}{d_0^3} = F \times \frac{T}{P_{\text{sat}}}, \quad (4)$$

where  $F$  is a multiplicative factor. Assuming this relationship, the dashed line in Fig. 3 is obtained by calculating the x-ray reflectivity from the thickness  $d$  of the film for the known  $q_z$ . Apart from normalization factors for the x-ray reflectivity,  $F$  and the equilibrium film thickness  $d_0$  are the only free parameters in the model. For small changes in the film thickness, the extent of thinning can be estimated from a model in which  $\Delta d = d - d_0$  is substituted in the left hand side of Eq. (4). The relative value of the parameter  $F$  in different data sets scales linearly with the x-ray intensity and  $^3\text{He}$  content in the cell. This model is also consistent with conventional reflectivity data (Fig. 1, Table I). In cases where the thinning is greater, the amplitude of the reflectivity oscillations is reduced, indicating that the film thickness varies over the footprint area.

### B. Films of pure $^3\text{He}$ and $^3\text{He}$ -rich $^3\text{He}/^4\text{He}$ mixtures

The behavior of pure  $^3\text{He}$  and  $^3\text{He}$ -rich mixtures is qualitatively the same as that of the mixtures described in the previous subsection. The extent of thinning is more severe and is significant even for strongly attenuated x-ray beams. For completeness, an example of a reflectivity measurement taken on pure  $^3\text{He}$  films with and without beam attenuator placed in front of the incident cryostat window is given in Fig. 4.

### C. Films of $^4\text{He}$ above the $\lambda$ point

X-ray induced thinning for  $^4\text{He}$  films above the superfluid transition  $T_\lambda = 2.17\text{K}$ , was observed by Lurio *et al.*<sup>5,2,3</sup> As part of this study, details of this thinning were investigated further. A typical plot of reflectivity vs. time on slow warm-up and cool-down is shown in Fig. 5. Thinning occurs within several milli-Kelvin on heating above the superfluid transition and is reversible. The time scale over which thinning occurs scales with the x-ray intensity and varies be-

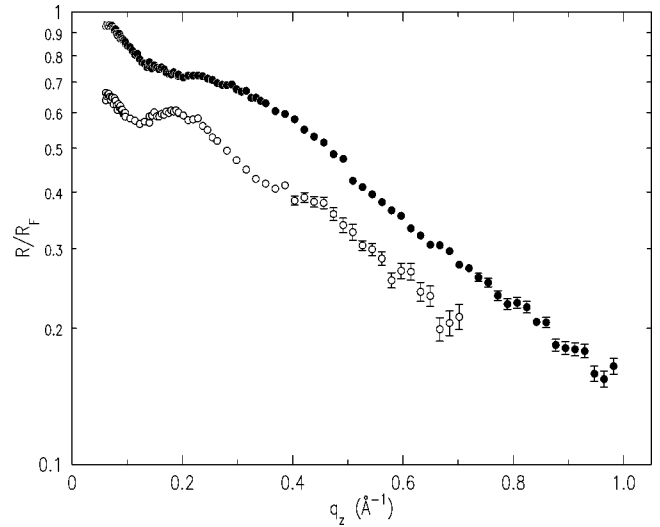


FIG. 4. Normalized reflectivity for a pure  $^3\text{He}$  film taken with different incident x-ray intensities. (●) Full beam; (○) beam attenuated by a  $10\times$  absorber. Data sets are offset for clarity. Film thickness is a function of  $q_z$  due to the changing footprint size.

tween 0.5 sec. at the synchrotron with full beam<sup>3</sup> and tens to hundreds of seconds either at the rotating anode facility or with significantly attenuated synchrotron radiation. Film thickness as a function of time for a film at  $T = 2.20\text{K}$  exposed to an attenuated x-ray beam is shown in Fig. 6.

## III. DISCUSSION

### A. Thinning models

Dramatic x-ray thinning of  $^4\text{He}$  films above the superfluid transition was first observed by Lurio *et al.*<sup>5,2,3</sup> The effect was explained as being caused by localized heating of the film. It was noted, however, that for the observed extent of thinning, a significant portion (50% or larger) of the entire beam energy would have to be deposited in the film itself despite the fact that nearly all x-ray photons are absorbed by the substrate. It was suggested that a substantial portion of primary photoelectrons escape the substrate and deposit their energy in the film and the vapor above it. Lack of heat exchange with the substrate was explained by a large Kapitza boundary resistance ( $\geq 800\text{ cm}^2\text{K W}^{-1}$ ) due to an exceptionally flat and clean substrate surface. Absence of thinning in superfluid  $^4\text{He}$  films could be naturally explained by thermal shorting by the superfluid flow of the film.

Subsequently it was found that significant x-ray-induced film thinning exists for  $^3\text{He}/^4\text{He}$  mixture films when such films are expected to be superfluid,<sup>6</sup> and an alternative explanation was required. It was suggested that primary photoelectrons ejected from the silicon substrate were attracted to the substrate by the positive ion charge left in silicon as well as by their image potential, and resided on the helium surface. Electrostatic pressure due to these charges leads to an increase in the chemical potential and hence reduces the film thickness. The two models are discussed below.

### B. X-ray induced electrostatic charging

In this model, the extent of thinning is determined by the equilibrium electron density at the helium surface. The equi-

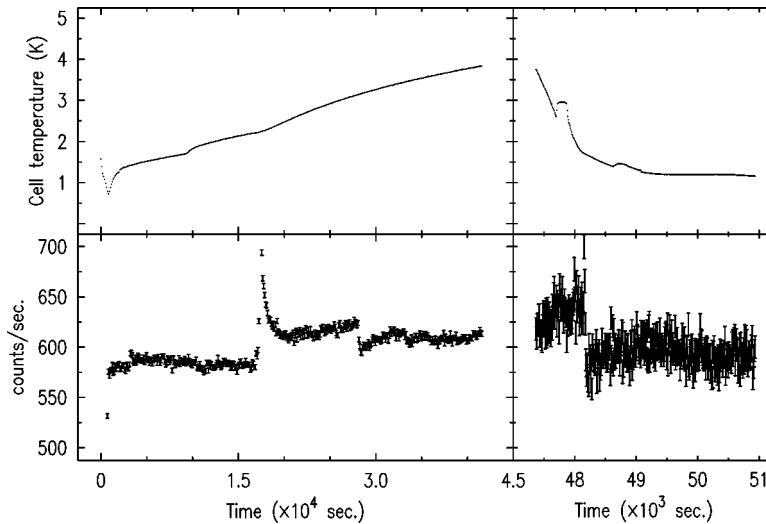


FIG. 5. Constant  $q_z$  warm-up and cool-down reflectivity for a  ${}^4\text{He}$  film. Reflectivity at a constant  $q_z = 0.068 \text{ \AA}^{-1}$  for slow warm-up and cool-down. Reflectivity oscillation at the  $\lambda$  point indicates thickness change from  $d \approx 140 \text{ \AA}$  to  $d \approx 50 \text{ \AA}$  over a time period of order  $2 \times 10^3$  sec. Data was taken at Harvard rotating anode facility.

librium is reached when the rate of the electron density dissipation (relaxation) becomes equal to the rate with which the electrons are generated. The rate of photoelectron production can be expected to be proportional to the number of incident x-ray photons, which is consistent with the observed linearity of the extent of thinning vs the x-ray intensity. Each primary photoelectron with an energy of  $\approx 10$  keV can create of the order of 400 additional free charges when it thermalizes through ionization. Since the ionization track length is a function of the vapor density, the total effective rate of electron production may also depend on the density of the helium vapor above the film. Although the source of charges

causing thinning seems clear, a credible model for the electron density relaxation is yet to be found. One possibility is that the electrons move along the film surface until they reach bare metal surface in the filling capillary. The relaxation rate would be determined by electron mobility along the surface. Another possibility is that there is a weak spot, a sharp protrusion, where electrons are capable of tunneling through the film. Relaxation is again limited by surface mobility. In still another model, upon reaching a critical density, a hydrodynamic instability develops,<sup>7,8</sup> allowing the electrons to break through the helium layer. The relaxation rate would depend on the surface tension.

The extent of thinning achieved in  ${}^4\text{He}$  films would require electron densities of the order of  $10^{11} \text{ cm}^{-2}$ .<sup>7</sup> The incident x-ray count for the thinning in Fig. 6 was  $1.05 \times 10^6$  photons/sec with the beam footprint area of  $\approx 0.1 \text{ cm}^2$ . Assuming secondary photoelectron production of 400 per each incident photon with all secondary electrons contributing to the thinning, the rate of the electron density increase would be  $\approx 4 \times 10^9 \text{ cm}^{-2} \text{ sec}^{-1}$ . This value is consistent with the observed rate of thinning to within an order of magnitude. The rates of thinning for  ${}^4\text{He}$  films exposed to larger x-ray flux at the synchrotron, observed by Lurio *et al.*<sup>3,2</sup> and in the current measurements, are found to be correspondingly higher. Another observation providing support to the electrostatic thinning hypothesis is that the typical recovery time for the  ${}^4\text{He}$  films above the  $\lambda$  point with the x-ray flux turned off is of the order of hours. After heating the cell to  $\geq 20$  K and cooling it again the film thickness recovers. This effect could be explained by the electrons tunneling through the film when the film thickness is reduced to  $\leq 10 \text{ \AA}$ .

The weakest point of this model is the discontinuity in thinning at the  ${}^4\text{He}$  superfluid transition. To explain the difference in the extent of thinning of less than  $0.5 \text{ \AA}$  at  $T < 2.17 \text{ K}$  with the highest x-ray flux at the synchrotron vs extreme thinning with the lowest flux at the rotating anode, the rates of relaxation have to differ by a factor of at least  $10^7$  across the  $\lambda$  point. Neither the surface tension nor the electron mobility have a discontinuity at the superfluid tran-

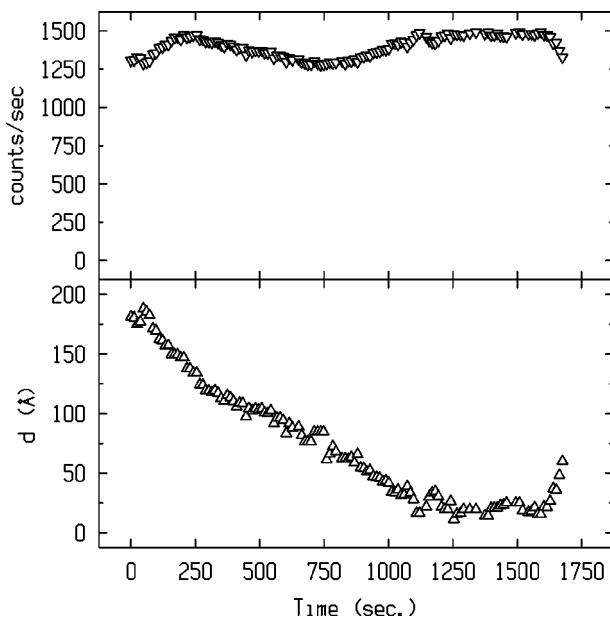


FIG. 6. Reflectivity at  $q_z = 0.050 \text{ \AA}^{-1}$  and corresponding film thickness vs time. The measurements were performed at the synchrotron with a strong attenuator in front of the cryostat. The temperature was maintained at  $2.20 \pm 0.01 \text{ K}$  during the measurement. The total incident x-ray flux corresponds to energy flux of  $0.00015 \text{ } \mu\text{W}$ . The x-ray shutter was opened at time  $t = 0$ .

sition (Ref. 9, and references therein). A similar argument arises in the case of  $^3\text{He}/^4\text{He}$  mixtures. Although the presence of  $^3\text{He}$  in the vapor phase would lower electron mobility, the latest measurements where the  $^3\text{He}$  content in the cell was kept constant and the film became thinner as the temperature was lowered indicate that scattering off  $^3\text{He}$  gas could not be the primary cause for the slowed relaxation. Apart from scattering from the gas, the surface electron mobility is limited due to the interaction with the surface modes. At temperatures above 0.4 K, where  $^3\text{He}$  atoms do not populate the surface state,<sup>10</sup> changes to the surface tension due to  $^3\text{He}$  are small. Direct interaction between the electrons and  $^3\text{He}$  quasiparticles is weak,<sup>11</sup> although additional surface modes may exist under certain conditions for larger  $^3\text{He}$  content.<sup>12</sup>

To further investigate the electrostatic charging hypothesis, the cell was equipped with electrodes to allow the application of electric fields across the substrate. Unfortunately, conducting substrates could not be used for unrelated technical reasons.<sup>1</sup> Although voltages corresponding to fields as high as  $2000\text{ V cm}^{-1}$  (limited by discharge in helium vapor) could be applied to the electrodes, the actual field at the substrate surface could not be determined. Even with this limitation, the setup would allow exploration of changes in thinning during transients, after the applied field was changed. An electron residing on the surface of a film  $100\text{ \AA}$  thick is subject to a field due to the image potential in the substrate of the order of  $10^4\text{ V/cm}$ .<sup>8</sup> If the thinning is caused by electron pressure, applying the field to reduce this pressure should thicken the film. For films thinned to  $30\text{--}50\text{ \AA}$  in cases of pure  $^3\text{He}$  and  $^4\text{He}$  above the superfluid transition, the available fields would be small in comparison with the image potential fields ( $\approx 10^5\text{--}10^6\text{ V cm}^{-1}$ ) and are unlikely to produce a measurable thickness change. However, in the case of dilute  $^3\text{He}/^4\text{He}$  mixtures the films in equilibrium are thicker and the image charge fields are smaller. We thus expected that the change in the extent of thinning due to applied field of  $1200\text{ V cm}^{-1}$ , assuming constant surface electron density, should be of the order of  $5\text{--}10\%$ . Since the equilibrium surface electron density is also a function of applied field, it should also change by a similar amount. Although the sensitivity of the reflectivity method is of the order of  $0.5\text{ \AA}$ , no additional change in film thickness was observed for the dilute mixture films thinned  $30\text{--}40\text{ \AA}$  by x rays, for both field polarities. An example of such a set of measurements is shown in Fig. 7.

The only case where the applied field appeared to have some effect on the film thickness was for the superfluid  $^4\text{He}$  films in the pressing geometry (substrate charged positively). Film thickness could be lowered by as much as  $120\text{ \AA}$  from an unperturbed thickness of  $\approx 230\text{ \AA}$  (see Fig. 8). Such variation in thickness would be consistent with the increased electron density at the surface as the secondary free electrons and ions in the vapor separate. This voltage-induced thinning was not reliably reproducible and may have been caused by a prior electric discharge in the cell.

### C. Thinning due to local heating

The disparity between thinning observed above the  $^4\text{He}$  superfluid transition and lack of such thinning below can be

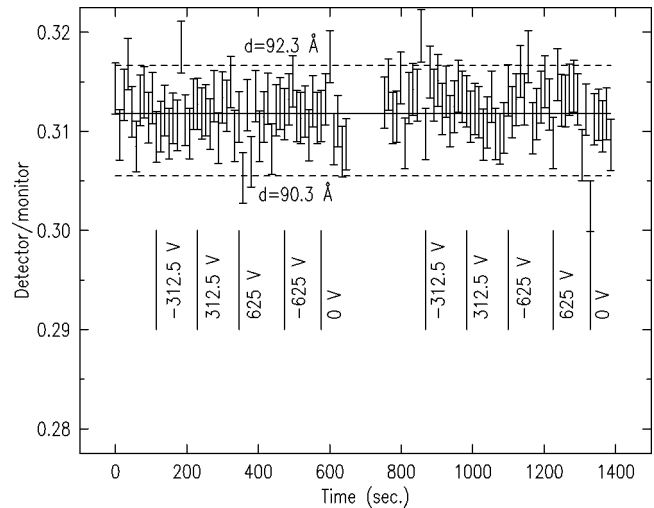


FIG. 7. Reflectivity at a constant  $q_z = 0.351\text{ \AA}^{-1}$  as a function of time for a  $^3\text{He}/^4\text{He}$  mixture film. Expected reflectivity for a film of  $91.3\text{ \AA}$  thick is shown as a solid line. Calculated reflectivities for films  $90.3$  and  $92.3\text{ \AA}$  are shown as dashed lines. Equilibrium film thickness  $d_0 \approx 125\text{ \AA}$ . Voltages are applied at the points shown. To convert voltages to field strengths, multiply by 2. Positive voltage indicates a positively charged substrate.

adequately explained by the local heating model.<sup>2,3</sup> The discussion below will attempt to show that such a model is also applicable to the case of superfluid  $^3\text{He}/^4\text{He}$  mixtures.

In the two-fluid model of a superfluid the superfluid fraction has zero entropy. In constricted geometries in general and in the case of helium films in particular any heat exchange requires mass transfer as well. Heat transfer in superfluid helium films has two distinct regimes. At higher temperatures, heat is carried away from a hot spot by the vapor, while the superfluid film flow replenishes the evaporated atoms. At lower temperatures, where the vapor pressure becomes negligible, heat transfer is primarily due to the capillary wave quasiparticles, or ripplons, and, in the case of  $^3\text{He}/^4\text{He}$  mixtures at  $T < 0.3\text{ K}$ , due to  $^3\text{He}$  quasiparticles bound to the surface.<sup>13</sup> In the former case the superfluid film flow is dissipation-free and for large enough thermal gradients is limited by the critical velocity at the spot with the shortest perimeter (this principle is the main idea behind superfluid film burners in cryostat design).

Until recently the description above was thought to be the case for the  $^3\text{He}/^4\text{He}$  mixtures as well, with  $^3\text{He}$  enriching the normal component in the two-fluid model. However, some experimental results indicate that the thermal conductance of  $^3\text{He}/^4\text{He}$  films is fundamentally different. Measurements of effective heat conductance along a coiled Mylar ribbon by Finotello *et al.*<sup>14</sup> show reduced conductance in the presence of  $^3\text{He}$  in thin ( $12$  and  $16\text{ \AA}$ )  $^4\text{He}$  films below the Kosterlitz-Thouless (KT) (Refs. 15 and 16) transition. This result is interpreted as an indication of free vortices present in the film even below the KT transition. Another measurement supporting this hypothesis is due to Ekholm and Hallock.<sup>17,18</sup> The superfluid persistent current decay rate was increased in the presence of  $^3\text{He}$  beyond what one would expect from the increase in the normal component in the two-fluid model.

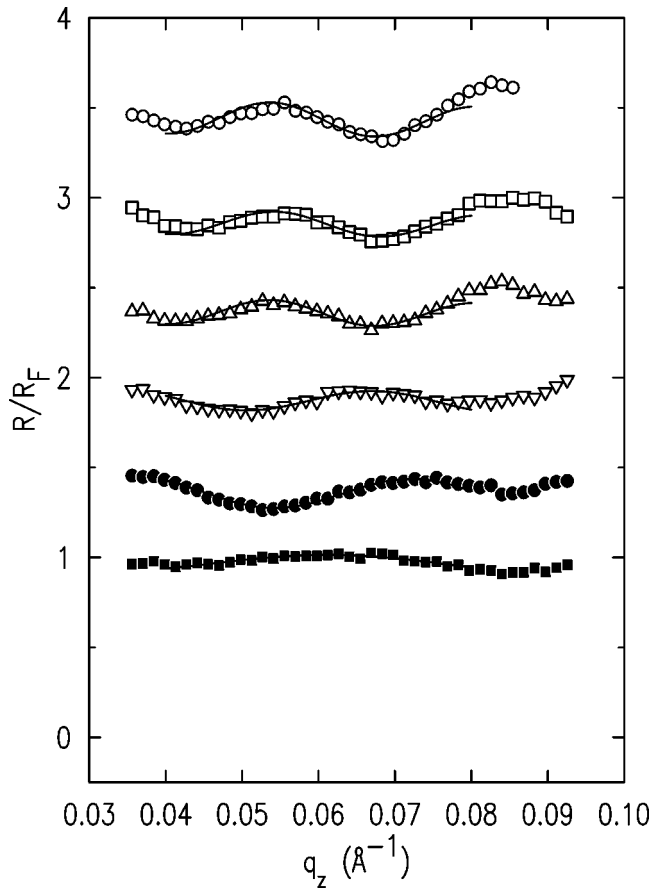


FIG. 8. Normalized reflectivity for a saturated superfluid  $^4\text{He}$  film on a highly doped silicon substrate for various applied voltages. (○)  $T=1.70$  K,  $U=-500$  V,  $d=233$  Å; (□)  $T=1.44$  K,  $U=0$  V,  $d=231$  Å; (△)  $T=1.25$  K,  $U=0$  V,  $d=234$  Å; (▽)  $T=1.18$  K,  $U=1$  V,  $d=186$  Å; (●)  $T=1.20$  K,  $U=10$  V,  $d=174$  Å; (■)  $T=1.90$  K,  $U=100$  V,  $d=102$  Å. Reflectivity data sets are offset for clarity. The typical error in the film thickness  $d$  is  $\pm 5$  Å. Film thickness changes are induced by applied fields as small as  $2$  V  $\text{cm}^{-1}$  (distance between the bias electrode and the substrate surface is  $\approx 5$  mm). Positive voltage indicates a positively charged substrate. The film is stable and of constant thickness for negative and zero voltages.

The motion of a free quantized vortex across the streamlines of potential flow introduces an energy loss mechanism.<sup>19</sup> The role of  $^3\text{He}$  impurity could be to reduce the energy necessary to create a vortex in the presence of superfluid flow,<sup>20,21</sup> or to facilitate vortex depinning. The case of  $^4\text{He}$ - $^3\text{He}$  films in the temperature range between 0.3 and 0.7 K differs from the case of bulk mixtures by the fact that the  $^3\text{He}$  bound to the vortices and carried away can be replenished from the vapor.

One has to note that the effect discussed above is different from the other  $^3\text{He}$ -induced reduction in the effective thermal conductance of  $^4\text{He}$  through refluxing. It is well known that adding small amounts of  $^3\text{He}$  into a cell which contains superfluid  $^4\text{He}$  and a fill capillary reduces the heat load. In this case,  $^3\text{He}$  in the gas phase impedes  $^4\text{He}$  vapor from fluxing back into the cell after evaporating at a higher temperature, and does not affect the film flow directly.

An estimate for the helium film flow rate can be inferred from the  $^3\text{He}/^4\text{He}$  mixture thinning data. The assumptions for

this calculation are as follows. As indicated by Lurio *et al.* for  $^4\text{He}$  thinning, of order 50% of the incident heat flux is dissipated in the film. We further assume that the film dissipates energy only by evaporating, without heat transfer to the substrate. The rate of atom loss  $dN/dt$  from the exposed area is

$$\frac{dN}{dt} = 0.5 \frac{WN_A}{L}, \quad (5)$$

where  $W$  is the incident energy flux,  $L$  is the helium molar latent heat and  $N_A$  is the Avogadro constant. Substituting  $W=2.9$   $\mu\text{W}$  and  $L \approx 80$  J  $\text{mol}^{-1}$ , we obtain the atom loss rate  $dN/dt$  of the order of  $10^{16}$   $\text{sec}^{-1}$ . From the incident slit settings and the incident angle the footprint perimeter is estimated to be a rectangle with length 10 mm and negligible width (0.4 mm). Under these assumptions, the helium film flow rate across the perimeter in equilibrium is calculated to be  $v \approx 0.2$   $\text{cm sec}^{-1}$ . In the absence of dissipation in film flow any two points along the flow path would have the same chemical potential  $\mu$ . In the presence of  $^3\text{He}$ , the thinning data suggests

$$\Delta\mu = f(N_{\text{film}})v \quad (6)$$

with the function  $f(N_{\text{film}})$  being linear in the  $^3\text{He}$  content  $N_{\text{film}}$  over at least 2 orders of magnitude. This result is consistent with the free vortex nucleation model in which the vortex production rate is linear in  $^3\text{He}$  content.

#### IV. CONCLUSION

X-ray induced thinning has been observed in films of pure  $^4\text{He}$  above the superfluid transition and in films of  $^3\text{He}/^4\text{He}$  mixtures. The extent of thinning in dilute  $^3\text{He}/^4\text{He}$  mixtures defined as the change in the local chemical potential is found to be linear in  $^3\text{He}$  concentration in the film over 2 orders of magnitude. The data is analyzed in terms of two models: local heating and electrostatic charging. The electrostatic charging model fails to explain the observed dramatic change in the extent of thinning at the  $^4\text{He}$  superfluid transition. The local heating model is consistent with the  $^4\text{He}$  data but requires that the film flow for  $^3\text{He}/^4\text{He}$  mixtures be dissipative. Dissipative flow for the mixture films has been previously observed in persistent current decay measurements,<sup>17,18</sup> and in heat conductivity measurements<sup>14</sup> and has been interpreted as being caused by free vortices persisting to temperatures below the superfluid transition. Our data also indicates that the observed dissipation is linear in  $^3\text{He}$  concentration.

#### ACKNOWLEDGMENTS

The authors acknowledge the assistance of Ralf Heilmann and Shilpa Jain in taking synchrotron data. This work was supported in part by NSF Grant No. NSF-DMR-95-23281. Research was carried out in part at the National Synchrotron Light Source, Brookhaven National Laboratory, which is supported by the U.S. Department of Energy, Division of Materials Sciences and Division of Chemical Sciences under Contract No. DE-AC02-98CH10886.

- \*Present address: UC Berkeley Physics Dept., Berkeley, CA 94720.
- <sup>1</sup>K. Penanen, M. Fukuto, R. K. Heilmann, I. F. Silvera, and P. S. Pershan, preceding paper, Phys. Rev. B **62**, 9621 (2000).
- <sup>2</sup>L. B. Lurio, T. A. Rabedeau, P. S. Pershan, Isaac F. Silvera, M. Deutsch, S. D. Kosowsky, and B. M. Ocko, Phys. Rev. B **48**, 9644 (1993).
- <sup>3</sup>L. B. Lurio, Ph.D. thesis, Harvard University, 1992.
- <sup>4</sup>G. K. White, *Experimental Techniques in Low-temperature Physics* (Oxford University Press, Oxford, 1987).
- <sup>5</sup>L. B. Lurio, T. A. Rabedeau, P. S. Pershan, I. F. Silvera, M. Deutsch, S. D. Kosowsky, and B. M. Ocko, Phys. Rev. Lett. **68**, 2628 (1992).
- <sup>6</sup>K. Penanen, P. S. Pershan, M. J. Regan, and I. F. Silvera, J. Low Temp. Phys. **101**, 489 (1995).
- <sup>7</sup>H. Etz, W. Gombert, W. Idstein, and P. Leiderer, Phys. Rev. Lett. **53**, 2567 (1984).
- <sup>8</sup>C. C. Grimes, Surf. Sci. **73**, 379 (1978).
- <sup>9</sup>Milton W. Cole, Rev. Mod. Phys. **46**, 451 (1974).
- <sup>10</sup>A. F. Andreev, Zh. Èksp. Teor. Fiz. **50**, 1415 (1966) [Sov. Phys. JETP **23**, 939 (1966)].
- <sup>11</sup>V. B. Shikin and Yu. P. Monarkha, Fiz. Nizk. Temp. **1**, 957 (1975) [Sov. J. Low Temp. Phys. **1**, 459 (1975)].
- <sup>12</sup>S. S. Sokolov, Guo-Qiang Hai, and Nelson Studart, Phys. Rev. B **55**, R3370 (1997).
- <sup>13</sup>I. B. Mantz, D. O. Edwards, and V. U. Nayak, Phys. Rev. Lett. **44**, 663 (1980).
- <sup>14</sup>D. Finotello, Y. Y. Yu, and F. M. Gasparini, Phys. Rev. Lett. **57**, 843 (1986).
- <sup>15</sup>J. M. Kosterlitz and D. J. Thouless, J. Phys. C **6**, 1191 (1973).
- <sup>16</sup>J. M. Kosterlitz, J. Phys. C **7**, 1046 (1974).
- <sup>17</sup>D. T. Ekholm and R. B. Hallock, Phys. Rev. B **21**, 3902 (1980).
- <sup>18</sup>D. T. Ekholm and R. B. Hallock, Phys. Rev. B **21**, 3913 (1980).
- <sup>19</sup>P. W. Anderson, Rev. Mod. Phys. **38**, 298 (1966).
- <sup>20</sup>J. C. Davis, J. Steinhauer, K. Schwab, Yu. M. Mukharsky, A. Amar, Y. Sasaki, and R. E. Packard, Phys. Rev. Lett. **69**, 323 (1992).
- <sup>21</sup>Y. M. Mukharsky, K. Schwab, J. Steinhauer, A. Amar, Y. Sasaki, J. C. Davis, and R. E. Packard, Physica B **194-196**, 591 (1994).